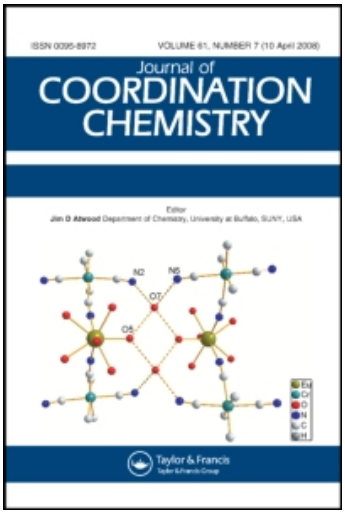

Journal of Coordination Chemistry
Publication details, including instructions for authors and subscription information:
http://www.informaworld.com/smpp/title~content=t713455674

Crystal structure, and thermal and magnetic properties of 2,4-dinitrobenzoatoterbium(III) complex

Sock-Sung Yun[a]; Youn-Bong Park[a]; Jeong-Ho Yeon[a]; Eun-Ju Kim[a]; Don Kim[b]
[a] Department of Chemistry, Chungnam National University, Daejeon, Republic of Korea [b] Department of Chemistry, Bukyung National University, Busan, Republic of Korea

First published on: 15 June 2007

To cite this Article Yun, Sock-Sung , Park, Youn-Bong , Yeon, Jeong-Ho , Kim, Eun-Ju and Kim, Don(2007) 'Crystal structure, and thermal and magnetic properties of 2,4-dinitrobenzoatoterbium(III) complex', Journal of Coordination Chemistry, 60: 24, 2703 — 2712, First published on: 15 June 2007 (iFirst)
To link to this Article: DOI: 10.1080/00958970701306231
URL: http://dx.doi.org/10.1080/00958970701306231

Journal of Coordination Chemistry
Vol. 60, No. 24, 15 December 2007, 2703–2712

Taylor & Francis
Taylor & Francis Group

Crystal structure, and thermal and magnetic properties of 2,4-dinitrobenzoatoterbium(III) complex

SOCK-SUNG YUN*†, YOUN-BONG PARK†,
JEONG-HO YEON†, EUN-JU KIM† and DON KIM‡

†Department of Chemistry, Chungnam National University,
Daejeon, 305-764, Republic of Korea
‡Department of Chemistry, Bukyung National University,
Busan, Republic of Korea

(*Received 10 September 2006; in final form 20 March 2007*)

The Tb(III) complex containing 2,4-dinitrobenzoate (2,4-DNB), $Tb(2,4\text{-}DNB)_3(H_2O)_2]\cdot C_2H_5OH$ has been synthesized and its crystal structure analyzed by X-ray diffraction methods. The complex crystallizes in the triclinic space group $P\bar{1}$, as a linear polymeric chain in which terbium ions are bridged by carboxylate groups. The eight-coordinate Tb ion with six carboxylate groups and two water molecules forms a slightly distorted square antiprism. Thermal and magnetic properties of the terbium complex were also studied.

Keywords: Terbium complex; Crystal structure; Thermal analysis; Magnetic measurements

1. Introduction

We have reported a series of lanthanide complexes of some high energy compounds, such as 3-nitro-1,2,4-triazolyl-5-one (NTO), 2,4,6-trinitrophenolate (picrate), and 2,6-dinitrophenolate (2,6-DNP) [1]. The crystal structures containing picrate have been thoroughly studied by Harrowfield *et al*. [2]. In studies of lanthanide complexes of nitro derivatives of phenol, it was found that the nitro groups play a significant role in complexation. The coordination behavior of 2,6-DNP is quite different from that of picrate. The absence of a nitro group at the *para* position on 2,6-DNP makes the nitro group *ortho* strongly involved in chelate formation [1(c)].

In order to find the role of nitro groups in the lanthanide complexation and the thermal explosion behavior of the nitro bezoates, we are now extending the study to complexation of nitro derivatives of benzoic acid. This article reports the crystal structure, and thermal and magnetic properties of the terbium complex containing 2,4-dinitrobenzoate (2,4-DNB), $[Tb(2,4\text{-}DNB)_3(H_2O)_2]\cdot C_2H_5OH$.

*Corresponding author. Tel.: +82 42 821 5478. Fax: +82 42 821 8893. Email: ssyun@cnu.ac.kr

Journal of Coordination Chemistry
ISSN 0095-8972 print/ISSN 1029-0389 online © 2007 Taylor & Francis
DOI: 10.1080/00958970701306231

2. Experimental

2.1. *Preparation and analysis of the complex*

The metal solution was prepared by dissolving terbium chloride ($TbCl_3 \cdot 6H_2O$, Aldrich 99.9%; ca 1 mmol) in water–ethanol mixture (1 : 1 volume ratio, 20 mL). The pH of the solution was adjusted to ca 2 with 7 M HNO_3 solution. The ligand solution was prepared by dissolving 2,4-dinitrobenzoic acid ($C_7H_4N_2O_6$, 3 mmol) in water–ethanol mixture (1 : 1 volume ratio, 30 mL) with stirring under the water bath at 60°C. The pH of the solution was adjusted to ca 6 with 3 M LiOH solution. The metal solution was added dropwise slowly to the ligand solution. The reaction mixture was stirred for 3 h at 60°C adjusting its pH to ca 3 and then cooling slowly to room temperature. Keeping the solution for a couple of days, colorless crystals of the complex precipitated. The complex is relatively stable in ambient conditions.

Chemical analysis of the complex was studied with a CE EA-1110 elemental analyzer. Anal. Calcd (%) for $C_{23}H_{19}N_6O_{21}Tb$: C, 31.60; H, 2.17; N, 9.62; O, 38.43. Found: C, 31.63; H, 1.81; N, 10.33; O, 38.27.

2.2. *X-ray crystallography*

The data for X-ray structure determination were collected on a Brucker AXS P4 X-ray diffractometer equipped with graphite monochromated Mo-Kα radiation ($\lambda = 0.71073$ Å) at 296 K. The unit cell dimensions were determined on the basis of 25 reflections in the range of $11.26^\circ < \theta < 13.07^\circ$. The data were collected by the $\omega - 2\theta$ scan mode. Stability of the crystal was monitored by measuring three standard reflections periodically (every 97 reflections) during the data collection. No crystal decay was observed. An empirical absorption correction based on 6ψ scans was applied to the data. The standard direct method was used to position the heavy atoms. The remaining non-hydrogen atoms were located from the subsequent difference Fourier synthesis. All non-hydrogen atoms were refined anisotropically. All hydrogen atoms were calculated in ideal positions and were riding on their respective carbon atoms ($B_{iso} = 1.2B_{eq}$). The structure was refined in full matrix least-square techniques provided in the SHELXTL [3] package of programs. The crystallographic data and detailed information of structure solution and refinement are listed in table 1.

2.3. *Thermal analysis*

The thermal decomposition of the complex was investigated on a Mettler–Toledo TGA 50 apparatus and Mettler–Toledo DSC model 821^e apparatus. The experimental procedure for thermal analysis is similar to that described previously [1].

2.4. *Magnetic property measurement*

Magnetic susceptibility measurements over the temperature range of 1.9 K to 300 K at 200 Oe were performed on a Quantum Design MPMS XL-7 SQUID magnetometer. Single crystals of $[Tb(2,4\text{-}DNB)_3(H_2O)_2] \cdot C_2H_5OH$ were manually selected for measurements and used without grinding as random oriented single crystals.

Table 1. Crystal data and structure refinement for $[Tb(2,4\text{-}DNB)_3(H_2O)_2]\cdot C_2H_5OH$.

Empirical formula	$C_{23}H_{19}N_6O_{21}Tb$
Formula weight	874.36
Temperature (K)	296(2)
Wavelength (Å)	0.71073
Crystal system	Triclinic
Space group	$P\bar{1}$
Unit cell dimensions (Å, °)	
a	9.1930(14)
b	13.1472(16)
c	13.9623(17)
α	108.557(8)
β	98.624(9)
γ	103.288(10)
Volume (Å^3)	1510.7(3)
Z	2
Calculated density (Mg m^{-3})	1.922
Absorption coefficient (mm^{-1})	2.446
$F(000)$	864
Crystal size (mm^3)	$0.40 \times 0.20 \times 0.04$
θ range for data collection (°)	1.86–25.00
Limiting indices	$-10 \le h \le 1$, $-14 \le k \le 14$, $-16 \le l \le 16$
Reflections collected/unique	6290/5216 [R (int) = 0.0246]
Completeness to $2(\theta) = 25.47°$	98.0%
Refinement method	Full-matrix least-squares on F^2
Data/restraints/parameters	5216/0/477
Goodness-of-fit on F^2	1.045
Final R indices [$I > 2\sigma(I)$]	$R_1 = 0.0269$, $wR_2 = 0.0671$
R indices (all data)	$R_1 = 0.0308$, $wR_2 = 0.0692$
Largest diff. peak and hole (e Å^{-3})	0.826 and −0.761

The data were corrected for diamagnetism of the constituent atoms using the values tabulated by Mulay [4]. Tb forms a slightly distorted square antiprism.

3. Results and discussion

3.1. *Crystal structure*

The terbium complex containing 2,4-DNB is a catenated polymeric compound whose stoichiometric chemical formula is $[Tb(2,4\text{-}DNB)_3(H_2O)_2]\cdot C_2H_5OH$, named *catena*-poly[[tetraaqua-1κ^2O,2κ^2O-tetrakis(μ-2,4-dinitrobenzoato-O:O')diterbium]-*bis*(μ-2,4-dinitrobenzoato-O:O')]diethanol]. Figure 1 shows perspective views of the complex, (a) a packing diagram and (b) a view through metal to metal axis (a-axis). As shown in figure 1, the complex has a one-dimensional chain structure in which the terbium ions are bridged alternatively by four and two 2,4-DNB ligands and two water molecules coordinate to each terbium ion. There is one ethanol in the outer coordination sphere of each terbium ion. Alternating distances between terbium ions are 4.203 Å and 5.045 Å, for tetrakis-bridged and *bis*-bridged, respectively. Intermolecular hydrogen bonds between para-nitro oxygens of one chain and coordinated water ligands of another chain; O(8)–H(41)$\cdots$O(15)$^{\#3}$ 2.911 Å, 157.4°, account for the weak interaction of the ortho-nitro group with the metal ion suggested in the IR study of lanthanide 2,4-dinitrobenzoates [5]. There are also intramolecular

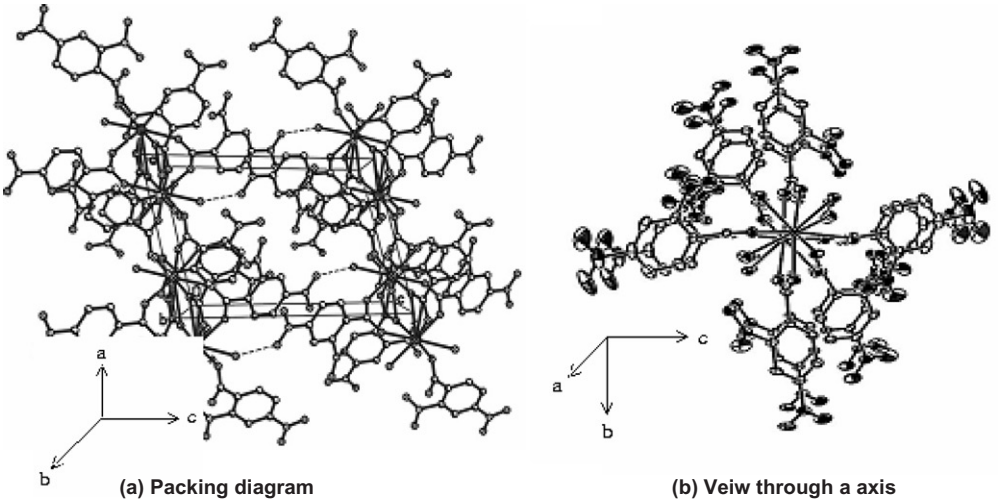

Figure 1. Perspective view of $[Tb(2,4\text{-}DNB)_3(H_2O)_2]\cdot C_2H_5OH$.

hydrogen bonds between ortho–nitro oxygens and coordinated water ligands, carboxylate oxygens and coordinated water ligands, and between coordinated water ligands, O(7)–H(42)···O(13)$^{\#1}$ 2.966 Å, 164.8°; O(7)–H(43)···O(2)$^{\#2}$ 2.925 Å, 111.9°; O(7)–H(43)···O(8)$^{\#2}$ 2.861 Å, 175.0°. These hydrogen bond interactions contribute to stabilization of the crystal structure.

The structure is basically similar to those of cerium and samarium complexes of 3,5-dinitrobenzoate [6]. Unlike lanthanide complexes of 2,6-dinitrophenol [1(c)], *ortho*-substituted nitro group of the benzene ring of the 2,4-DNB complex does not play an important role in coordination. Instead, the *ortho*-nitro group in the 2,4-DNB complex is excluded from coordination to the metal by the bridging power of the carboxylate group, constructing the polymeric chain structure. Complexes of lanthanum and samarium nicotinates show the dimeric structure in which the carboxylate group of the terminal ligands is bidentate while the carboxylate group of the bridging ligands is ambidentate [7]. Perhaps the basicity of nicotinate is strong enough to stabilize the four-membered chelate ring, while the basicities of 3,5- and 2,4-dinitrobenzoates are too weak to be a bidentate chelate ligand. Dinitrobenzoic acids are ambidentate to bridge metal ions within the polymeric chain. The pKa values of nicotinic acid, 3,5-dinitrobenzoic acid, and 2,4-dinitrobenzoic acid are 4.73, 2.82, and 1.43, respectively [8]. The basicity of nicotinate is the highest among the three ligands.

Selected bond lengths and angles for terbium 2 4-dinitrobezoate are listed in table 2. An ORTEP diagram of the molecular structure for the complex is presented by the atomic numbering scheme in figure 2. As shown in figures 1(b) and 2, in the space between tetrakis-bridged terbium ions, the bridging ligands form two planes approximately perpendicular. Each plane is formed by two carboxylate groups and two metal ions. The dihedral angle formed by vertical (on *a–b* plane) and horizontal (on *a–c* plane) planes is 87.38°. The plane formed by the two carboxylate groups and the two metal ions in the space between *bis*-bridged terbium ions (Tb–Tb$^{\#2}$), bisects the dihedral angle made by the vertical and horizontal planes. The bisecting angle is 42.44°.

Each Tb(III) is coordinated to oxygen atoms of six carboxylate ligands and oxygen atoms two water ligands. The Tb–O_{water} bond distances are within the range

Table 2. Selected bond lengths (Å) and angles (°) for $[Td(2,4\text{-}DNB)_3(H_2O)_2]\cdot C_2H_5OH$.

Tb–O(6)	2.304(3)	C(7)–C(8)	1.388(5)
Tb–O(2)	2.305(3)	C(7)–C(20)	1.519(5)
Tb–O(4)	2.386(3)	C(8)–N(3)	1.469(5)
Tb–O(1)	2.411(2)	C(20)–O(4)	1.248(5)
Tb–O(5)	2.415(3)	C(20)–O(1)$^{\#1}$	1.250(4)
Tb–O(3)	2.430(3)	N(3)–O(14)	1.220(5)
Tb–O(7)	2.449(3)	N(3)–O(13)	1.221(5)
Tb–O(8)	2.512(3)	C(13)$^{\#3}$–C(14)$^{\#3}$	1.397(5)
Tb–O(6)$^{\#1}$	2.869(3)	C(13)$^{\#3}$–C(21)	1.510(5)
Tb$^{\#1}$–O(6)$^{\#1}$	2.304(3)	C(14)$^{\#3}$–N(5)$^{\#3}$	1.474(6)
C(1)–C(19)	1.503(5)	C(21)–O(2)$^{\#2}$	1.237(5)
C(1)–C(2)	1.383(6)	C(21)–O(5)	1.247(5)
C(2)–N(1)	1.462(7)	N(6)$^{\#3}$–O(19)$^{\#3}$	1.173(7)
C(19)–O(3)	1.238(5)	N(6)$^{\#3}$–O(20)$^{\#3}$	1.213(7)
C(19)–O(6)$^{\#1}$	1.251(5)		
N(1)–O(9)	1.204(6)		
N(1)–O(10)	1.216(6)		
O(6)–Tb–O(2)	146.61(10)	O(6)–Tb–O(3)	119.68(10)
O(6)–Tb–O(4)	73.42(10)	O(2)–Tb–O(3)	78.43(10)
O(2)–Tb–O(4)	139.52(10)	O(4)–Tb–O(3)	82.92(10)
O(6)–Tb–O(1)	76.58(10)	O(1)–Tb–O(3)	78.04(10)
O(2)–Tb–O(1)	80.88(9)	O(5)–Tb–O(3)	138.17(10)
O(4)–Tb–O(1)	129.65(9)	O(6)–Tb–O(6)$^{\#1}$	71.82(10)
O(6)–Tb–O(5)	86.30(10)	O(2)–Tb–O(6)$^{\#1}$	120.62(9)
O(2)–Tb–O(5)	97.60(9)	O(4)–Tb–O(6)$^{\#1}$	65.93(9)
O(4) –Tb–O(5)	73.50(9)	O(1)–Tb–O(6)$^{\#1}$	66.73(9)
O(1)–Tb–O(5)	143.09(10	O(5)–Tb–O(6)$^{\#1}$	137.80(9)
		O(3)–Tb–O(6)$^{\#1}$	47.90(8)

$^{\#1}$ $-x+2, -y+1, -z+2$; $^{\#2}$ $-x+3, -y+1, -z+2$; $^{\#3}$ $-x+2, -y+1, -z+1$.

of 2.449(3)–2.512(3) Å which are a little longer than the sum of the covalent radii of the Tb and O atoms (2.42°). The Tb–O distances to the carboxylate groups are in the range of 2.304(3)–2.429(3) Å, which are a little shorter than the Tb–O_{water} bond distances. Thus, the skeletal structure around the Tb atom forms a slightly distorted square antiprism.

The most notable observation in this complex is that some of the 2,4-dinitrobenzoate ligands may be considered as terdentate, as shown in figure 2. In the 2,4-dinitrobenzoate ligands placed on the horizontal plane, one oxygen in each carboxylate group is bound to one metal ion, whereas another oxygen interacts very weakly with two metal ions. The former oxygen O(3) of the carboxylate is 2.429(3) Å from Tb. The latter oxygen of the carboxylate O(6)$^{\#1}$ is 2.304(3) Å from Tb$^{\#1}$ and 2.869(3) Å from Tb. Similar observations have been reported for the lanthanum nicotinate complex, in which one oxygen of the carboxylate group is bound to metal ions in 2.51 Å and 2.92 Å distances, respectively [7].

3.2. *Thermal analysis*

The thermograms of TG-DTG and DSC of 2,4-DNB and its terbium complex $[Tb(2,4\text{-}DNB)_3(H_2O)_2]\cdot C_2H_5OH$ were obtained with linear temperature increase.

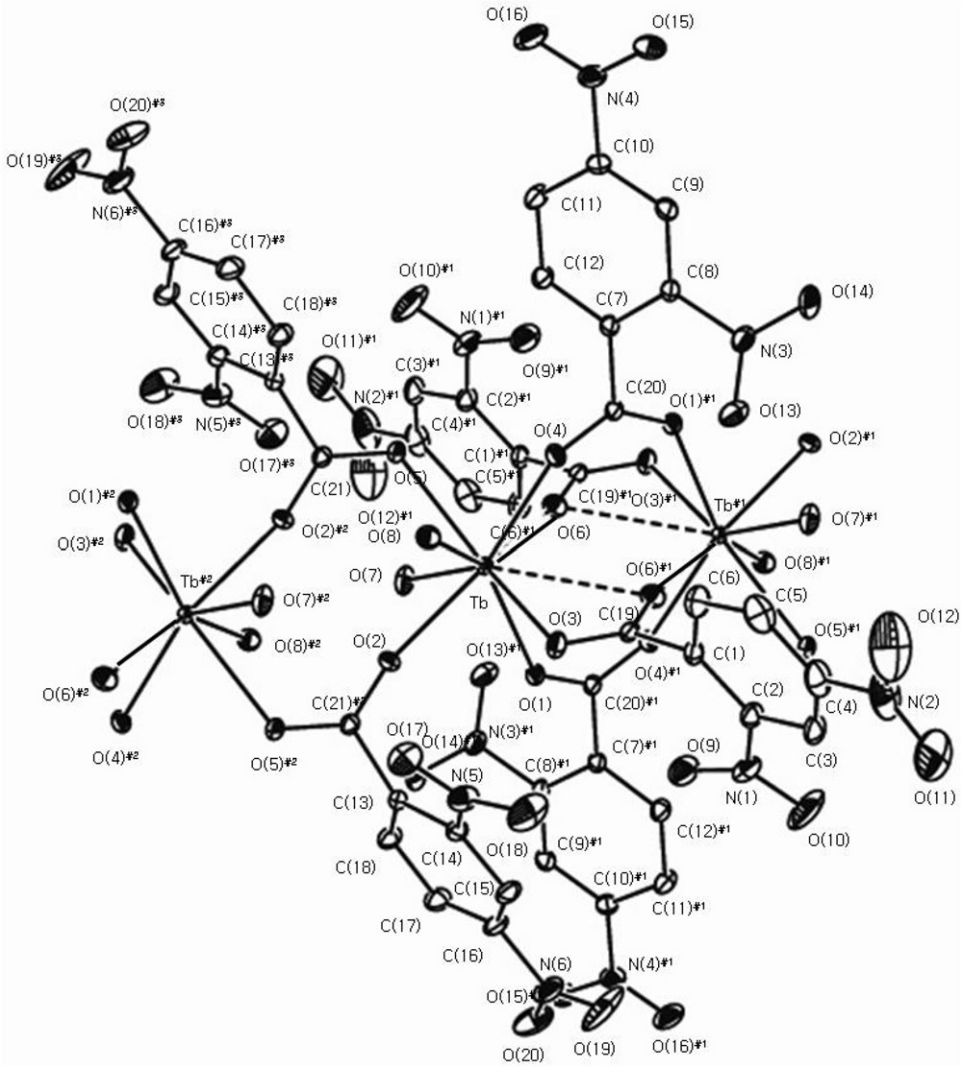

Figure 2. Molecular structure of $[Tb(2,4\text{-}DNB)_3(H_2O)_2]\cdot C_2H_5OH$.

TG-DTG curves for 2,4-DNB indicate that it decomposes thermally in one step around 195–290°C. However, the curve also shows gradual mass loss till 450°C. DSC curve for the thermal decomposition of 2,4-DNB displays two endothermic and one exothermic peaks, one sharp endothermic peak for the phase change at 180°C and the broad endothermic peak for decomposition around 300°C followed immediately by the broad exothermic peak for the explosion.

Figure 3 shows the TGA and DSC thermograms of the complex. The thermal analysis data indicate that the thermal decomposition of the terbium complex $[Tb(2,4\text{-}DNB)_3(H_2O)_2]\cdot C_2H_5OH$ occurs in three stages under the experimental conditions, desolvation of ethanol from outer sphere, dehydration of coordinated water molecules, and decomposition of the complex to the metal oxides through explosion.

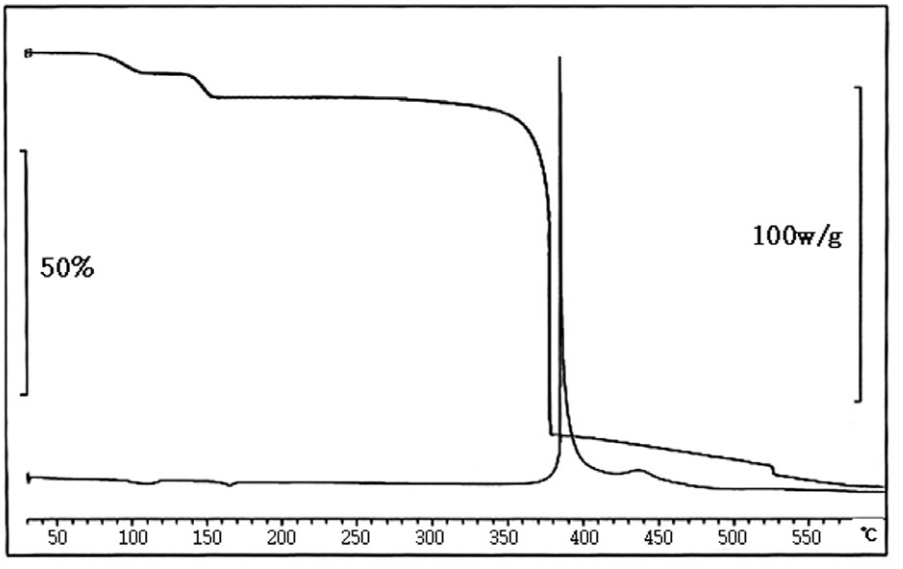

Figure 3. TGA and DSC thermograms for $[Tb(2,4\text{-}DNB)_3(H_2O)_2]\cdot C_2H_5OH$.

TG-DTG curves show mass loss of 4.3% (Calcd 5.3%) for ethanol desolvation between 72 and 110°C, a weight loss of 4.9% (Calcd 4.1%) for dehydration of coordinated water ligands between 140–156°C, and mass loss of 79.4% (Calcd 69.2%, assuming the formation of Tb_4O_7 as the residue) for decomposition with the explosion of Tb(2,4-DNB)$_3$ between 270–550°C. The mass loss at final stage shows about 10% discrepancy to the calculated value. This discrepancy may be caused by the residue being blown off partly by the explosion.

DSC curve for the complex shows two small endothermic peaks centered at 109 and 165°C, and one sharp exothermic peak with a maximum temperature at 384.8°C accompanying a medium size shoulder at 440°C. The former correspond to desolvation of the ethanol and decoordination of water ligands. Desolvation and decoordination enthalpies determined from DSC data are ca $\Delta H_{EtOH} = 92.3\,kJ\,mol^{-1}$ and ca $\Delta H_W = 63.0\,kJ\,mol^{-1}$, respectively. The peak around 400°C corresponds to decomposition of the complex with explosion. The enthalpy of decomposition calculated from the peak area is ca $\Delta H_{dec} = -3823.2\,kJ\,mol^{-1}$. The exothermic peak for the explosion of the highly energetic compound 2,4-TNB becomes sharp and intense in a narrow temperature range in the terbium complex, as has similarly observed for the lanthanide complexes containing picrate and 2,6-dinitrophenolate [1]. Explosion of coordinated ligands are impacted by the nature of the complexes.

3.3. *Magnetic property*

Figure 4 shows the magnetic hysteresis curve at 1.9 K and 300 K. In both temperatures, the magnetization M depends linearly on applied magnetic filed H at low field, <0.5 T. The linear M–H relationship was also observed at other temperatures. This linear dependence of magnetization justifies the evaluation of a susceptibility $\chi = M/H$ to describe the paramagnetic behavior of the sample in the linear region [9].

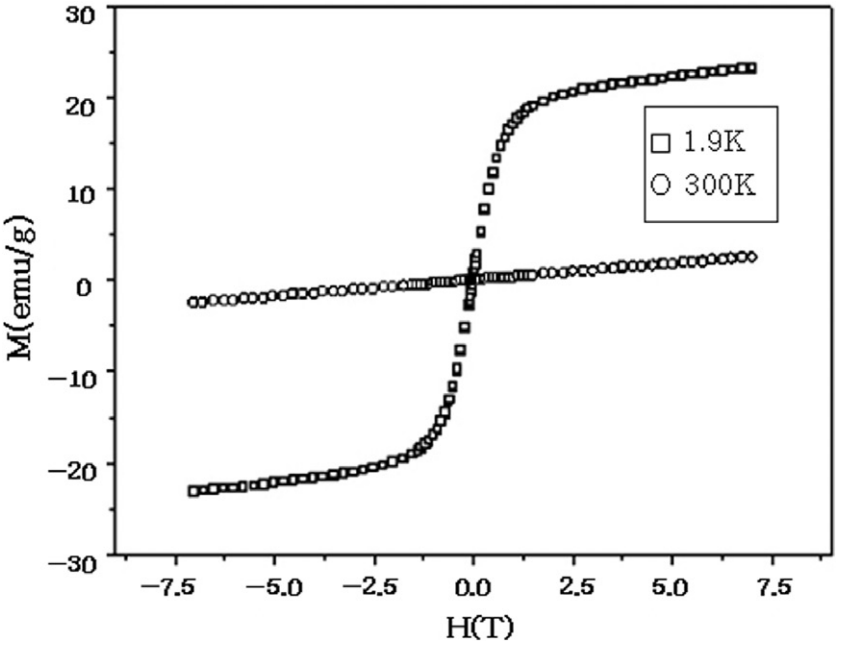

Figure 4. Magnetic hysteresis curve at 1.9 K and 300 K.

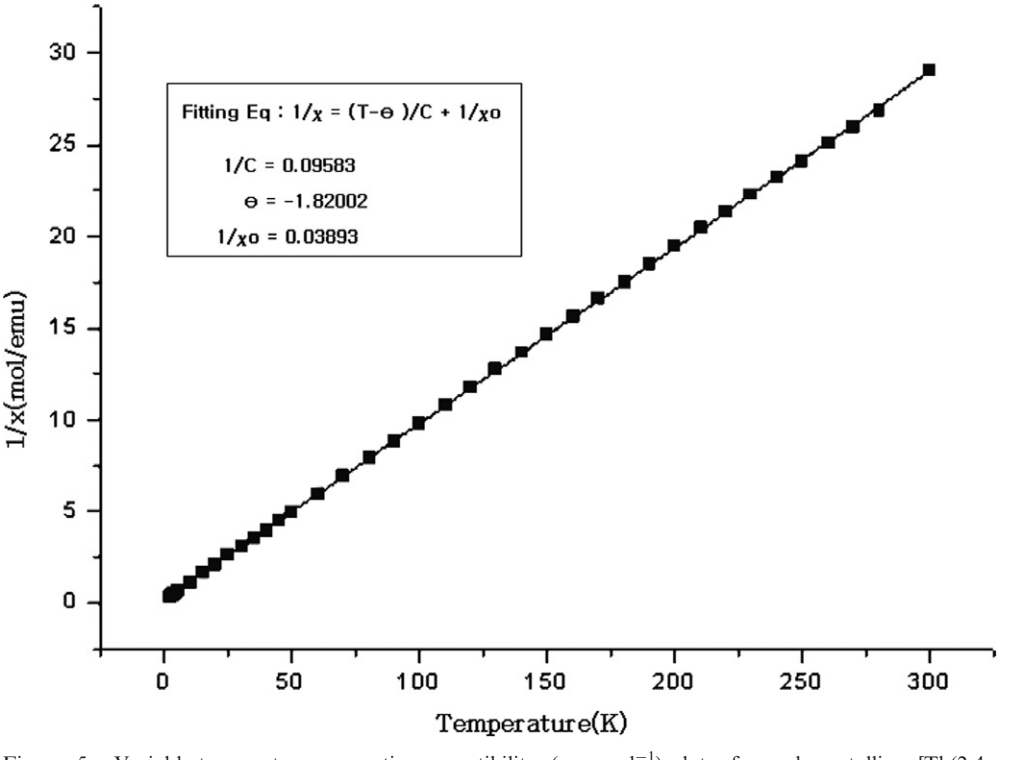

Figure 5. Variable-temperature magnetic susceptibility (emu mol^{-1}) data for polycrystalline $[Tb(2,4\text{-}DNB)_3(H_2O)_2]\cdot C_2H_5OH$.

Figure 5 shows the inverse susceptibility ($1/\chi$) as a function of temperature (T) which fits the Curie–Weiss law. The χ was evaluated in a magnetic field $H = 200$ Oe. The line in the plot indicates the fit to the Curie–Weiss law;

$$\frac{1}{\chi} = \frac{(T-\theta)}{C} + \frac{1}{\chi_o}$$

where θ is the Weiss temperature, C is Curie constant, and χ_o is the temperature independent contribution (TIC) to susceptibility (diamagnetism of core electron and temperature-independent paramagnetism, etc.). The perfect linear relationship (linear correlation coefficient $R = 1.000$) in the plot indicates that the sample is paramagnetic in the entire range of temperature. The other parameters (Weiss temperature $= -1.82$ K and $1/\chi_o = 0.039$ mol emu^{-1}) are negligible. Therefore, we assume the fit obeys the Curie law. The Curie constant $C = 10.43$ emu K mol^{-1}, evaluated from the slope ($1/C$) of the fit, is related to the effective magnetic moment (μ_{eff}) [10]. $C = 0.125\ \mu_{eff}^2$ (in Bohr Magneton: BM). Therefore, the observed effective magnetic moment can be evaluated, $\mu_{eff(obs)} = 9.41$ BM.

Even though the spin only coupling is satisfactory to estimate the effective magnetic moment $\mu_{eff(cal)}$ of most iron series elements, the *jj* coupling is important to estimate $\mu_{eff(cal)}$ for heavy elements such as other lanthanides; $\mu_{eff(cal)} = g_J[(J(J+1)]^{1/2}$ [11]. Because there is one $Tb^{3+}(4f^8, {}^7F_6)$ per asymmetric unit, the $\mu_{eff(cal)}$ can be easily calculated using evaluated Lande constant ($g_J = 1.5$) as $\mu_{eff(cal)} = 9.72$ BM. This is not far from the observed effective magnetic moment and suggests stable Tb^{3+} ions in this compound, free from any magnetic interactions.

Supplementary material

Complete lists with atomic coordinates, anisotropic displacement parameters, bond lengths and angles have been deposited at Cambridge Crystallographic Data Center, 912 Union Road, Cambridge CB2 1EZ, UK [CCDC 616045].

Acknowledgements

This work was supported by a grant (No. R01-2001-00055) from Korea Science and Engineering Foundation.

References

[1] (a) S.-S. Yun, J.-K. Kim, C.-H. Kim. *J. Alloys Compd.*, **408–412**, 945 (2006); (b) S.-S. Yun, S.K. Kang, H.-R. Suh, H.-S. Suh, E.K. Lee, J.-K. Kim, C.-H. Kim. *Bull. Korean Chem. Soc.*, **26**, 1197 (2005) 1197; (c) S.-S. Yun, H.-R. Suh, H.-S. Suh, S.K. Kang, J.-K. Kim, C.-H. Kim. *J. Alloys Compd.*, **408–412**, 1030 (2006).

[2] (a) J.M. Harrowfield, L. Weimin, B.W. Skelton, A.H. White. *Aust. J. Chem.*, **47**, 321 (1994); (b) J.M. Harrowfield, L. Weimin, B.W. Skelton, A.H. White. *Aust. J. Chem.*, **47**, 339 (1994); (c) J.M. Harrowfield, L. Weimin, B.W. Skelton, A.H. White. *Aust. J. Chem.*, **47**, 349 (1994); (d) J.M. Harrowfield, B.W. Skelton, A.H. White. *Aust. J. Chem.*, **47**, 349 (1994).

[3] G.M. Sheldrick. *SHELXTL NT Version 6.12; Bruker Analytical X-ray Instruments*, Inc., Madison, WI (2000).

[4] L.N. Mulay. In *Theory and Applications of Molecular Paramagnetism*, E.A. Boudreaux, L.N. Mulay (Eds), p. 494, 495, New York, Wiley (1976).
[5] W. Ferenc. *Monatsh. Chem.*, **120**, 539 (1989).
[6] (a) M.N. Tahir, D. Ulku, C. Unaleroglu, E.M. Movsumov. *Acta Cryst.*, **C52**, 1449 (1996); (b) C. Arici, D. Ulku, M.N. Tahir, C. Unaleroglu. *Acta Cryst.*, **C55**, 198 (1996).
[7] J.W. Moore, M.D. Glick, W.A. Baker Jr. *J. Amer. Chem. Soc.*, **87**, 1611 (1965).
[8] (a) *CRC Handbook of Chemistry and Physics*, 76th Ed. CRC Press, New York (1995); (b) G. Kortum, W. Vogel, K. Andrussow. *Dissociation Constants of Organic Acids in Aqueous Solution*, Butterworth, London (1961); (c) A. Albert, E.P. Serjeant. *Determination of Ionization Constants, A Laboratory Manual*, 3rd Edn, Chapman and Hall, London (1984).
[9] X. Shen, Y. Ding, J. Liu, Z. Han, J.I. Budnick, W.A. Hines, S.J. Suib. *J. Am. Chem. Soc.*, **127**, 6166 (2005).
[10] Z.S. Teweldemedhin, R.L. Fuller, M. Greenblatt. *Chem. Edu.*, **73**(9), 906 (1996).
[11] R.L. Carlin. *Magneto Chemistry*, Spring-Verlag, Berlin (1986).